Tuning the electronic properties of the golden buckyball by endohedral doping: $M@Au_{16}^-$ (M=Ag,Zn,In)

Lei-Ming Wang,[1] Rhitankar Pal,[2] Wei Huang,[1] Xiao Cheng Zeng,[2,a)] and Lai-Sheng Wang[1,b)]
[1]*Department of Physics, Washington State University, 2710 University Drive, Richland, Washington 99354, USA and Chemical and Materials Sciences Division, Pacific Northwest National Laboratory, MS K8-88, P. O. Box 999, Richland, Washington 99352, USA*
[2]*Department of Chemistry and Center for Materials and Nanoscience, University of Nebraska-Lincoln, Lincoln, Nebraska 68588, USA*

(Received 2 November 2008; accepted 5 January 2009; published online 4 February 2009)

The golden Au_{16}^- cage is doped systematically with an external atom of different valence electrons: Ag, Zn, and In. The electronic and structural properties of the doped clusters, MAu_{16}^- (M=Ag,Zn,In), are investigated by photoelectron spectroscopy and theoretical calculations. It is observed that the characteristic spectral features of Au_{16}^-, reflecting its near tetrahedral (T_d) symmetry, are retained in the photoelectron spectra of MAu_{16}^-, suggesting endohedral structures with little distortion from the parent Au_{16}^- cage for the doped clusters. Density functional calculations show that the endohedral structures of $M@Au_{16}^-$ with T_d symmetry are low-lying structures, which give simulated photoelectron spectra in good agreement with the experiment. It is found that the dopant atom does not significantly perturb the electronic and atomic structures of Au_{16}^-, but simply donate its valence electrons to the parent Au_{16}^- cage, resulting in a closed-shell 18-electron system for $Ag@Au_{16}^-$, a 19-electron system for $Zn@Au_{16}^-$ with a large energy gap, and a 20-electron system for $In@Au_{16}^-$. The current work shows that the electronic properties of the golden buckyball can be systematically tuned through doping. © *2009 American Institute of Physics*. [DOI: 10.1063/1.3073884]

Gold and doped gold clusters have attracted increasing research interests, stimulated primarily by the discovery of unique catalytic properties of supported gold nanoparticles.[1] During a recent photoelectron spectroscopy (PES) and density functional theory (DFT) study of the structures of Au_n^- clusters,[2] Au_{16}^- was found to be a highly stable hollow cage cluster with a large internal volume analogous to the fullerenes.[3] The diameter of the Au_{16}^- cage (the golden buckyball) was shown to be ~5.5 Å,[2] suggesting possible endohedral doping to form a new class of golden cages with tailored properties similar to the endohedral fullerenes.[4] This study spurred immediate theoretical interests, suggesting possible endohedral doping by a Si and Al atom,[5] or a Mg atom.[6]

The first endohedrally doped golden cage was observed for $Cu@Au_{16}^-$,[7] in which the Cu atom was shown to reside inside the Au_{16}^- cage with little structural distortion. The Cu atom was observed to donate its valence electron to the cage, yielding a stable closed-shell 18-electron system for $Cu@Au_{16}^-$. In contrast to the previous theoretical suggestion,[5] however, our joint PES and DFT studies revealed that Si, as well as Ge and Sn, cannot be doped into the golden cage.[8] Instead, the MAu_{16}^- (M=Si,Ge,Sn) clusters were shown to be exohedral, where the tetrahedral golden cage is completely distorted due to the strong M-Au local interactions. The unusual structure of the $SiAu_{16}^-$ cluster was also reached by a theoretical study by Sun *et al.*[9] In another theoretical study, Sun *et al.*[10] also investigated the Au_{16} cage doped by a W atom and found that the resulting WAu_{16} cluster is distorted to a $W@Au_{12}$ unit plus four additional Au atoms on the outside. The $W@Au_{12}$ cluster was predicted previously by Pyykkö and Runeberg[11] to be a highly stable 18-electron icosahedral cluster and was confirmed experimentally.[12] The result for the WAu_{16} cluster again indicates that the local dopant-Au interactions determine the ultimate structures and stability of the doped Au_{16}^- clusters. A more recent theoretical study suggested that Li and Na atom can be doped into the Au_{16}^- cage, while Ag and K cannot be doped inside because of their larger atomic size.[13]

It is important to understand what kind of atoms can be doped inside the golden buckyball. The previous studies suggest that metallic atoms, such as Cu, can be doped inside the golden cage and the dopant atom transfers its valence electron to the cage to create a charge transfer complex, $Cu^+@Au_{16}^{2-}$. On the other hand, strong dopant-Au interactions, such as for Si or W dopant, tend to destroy the Au_{16} cage and lead to new types of structures. Interestingly, these observations are quite similar to the doped fullerenes. It is known that only alkali, alkali earth, or rare earth atoms can be doped inside the fullerenes to form charge transfer complexes,[14] whereas transition metals do not form endohedral fullerenes due to the strong M-C interactions that lead to metal carbides.

In the current work, we investigate the doping of the golden cage by three metal atoms, Ag, Zn, and In, which

a)Electronic mail: xczeng@phase2.unl.edu.
b)Electronic mail: ls.wang@pnl.gov.

possess different numbers of valence electrons. The inclusion of Ag also allows us to examine the effects of dopant size by comparing with our previous work on $Cu@Au_{16}^-$. Our results show that all three elements can be doped into the Au_{16}^- cage to form highly stable endohedral $M@Au_{16}^-$ clusters with little distortion to the parent cage. We further show that the interactions between the dopant atoms and the golden cage can be viewed as charge transfer from the dopant to the cage, demonstrating that the electronic structure of the golden cage can be tuned systematically by changing the dopant atom with different valence electrons.

The experiment was performed using a magnetic-bottle PES apparatus equipped with a laser vaporization cluster source.[15] The MAu_{16}^- (M=Ag,Zn,In) clusters were produced by laser vaporization of Au/M composite disk targets containing about 7% Ag, 8% Zn, and 4% In, respectively. Negatively charged clusters were extracted from the cluster beam and analyzed using a time-of-flight mass spectrometer. The MAu_{16}^- clusters were selected and decelerated before being photodetached by a 193 nm (6.424 eV) laser beam from an ArF excimer laser. The photoelectron spectra were calibrated using the known spectra of Au^-. The electron energy resolution of the apparatus was $\Delta E/E \sim 2.5\%$, i.e., about 25 meV for 1 eV electrons.

Our theoretical study began with unbiased searches for the low-lying structures of MAu_{16}^- (M=Ag,Zn,In) using the basin-hopping optimization technique[16–18] coupled with DFT geometric optimization within the generalized gradient approximation in the Perdue–Burke–Ernzerhof (PBE) functional form[19] using the DMOL3 DFT program.[20] About 200 structural isomers were generated for each cluster. The top 20–30 isomers were reoptimized using the "PBEPBE" functional[19] with a scalar relativistic effective core potential LANL2DZ basis set,[21] implemented in the GAUSSIAN03 program.[22] Harmonic vibrational frequencies were calculated to confirm that the low-lying isomers are true minima. Single-point energies of the corresponding neutral isomers in the anion geometries were calculated to evaluate the first vertical detachment energy (VDE) of the anion isomers. The binding energies of deeper orbitals were added to the first VDE to give the VDEs of the excited states. Each calculated VDE was fitted with a Gaussian width of 0.06 eV to yield the simulated PES spectra.

Figure 1 displays the photoelectron spectra of the three MAu_{16}^- clusters, along with that of Au_{16}^- for comparison. The spectrum of $AgAu_{16}^-$ [Fig. 1(b)] is similar to that of Au_{16}^- with three well-resolved peaks in the low binding energy range between 4.1 and 4.8 eV followed by a large energy gap and more congested spectral features beyond 5.5 eV. The spectra of $ZnAu_{16}^-$ and $InAu_{16}^-$ are similar to that of $AgAu_{16}^-$ except an extra low binding energy feature (X) in the doped clusters. We note that the low binding energy band X in the $InAu_{16}^-$ spectrum [Fig. 1(d)] has a higher electron binding energy than that in $ZnAu_{16}^-$ and is also more intense. The weak features denoted with "*" in the spectra of MAu_{16}^- are either due to impurities or weakly populated isomers. The VDEs of the ground state bands for the three MAu_{16}^- clusters are given in Table I and compared to the theoretical values.

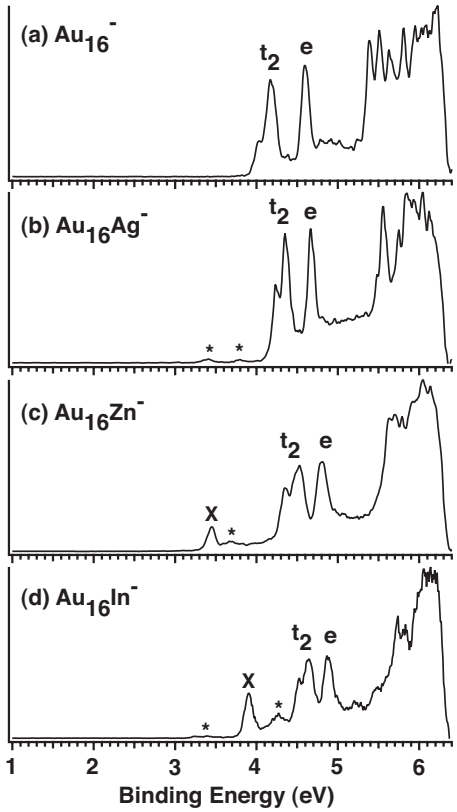

FIG. 1. Photoelectron spectra of the doped golden cages $Au_{16}M^-$ (M=Ag,Zn,In) at 193 nm, compared to that of Au_{16}^-.

As discussed previously,[2,7] the Au_{16}^- spectrum is unique: It has a very high electron binding energy and does not exhibit a large energy gap like other even-sized gold clusters,[23–25] which is because the tetrahedral Au_{16} cage is open shell with two unpaired electrons and two extra electrons are needed to make a closed-shell 18-electron Au_{16}^{2-} cage. Walter and Hakkinen[5] used the electron shell model to rationalize the high stability of the Au_{16}^{2-} cage with three filled electron shells, $1s^21p^61d^{10}$. The $1d$ shell transforms into t_2 and e molecular orbitals (MOs) under the T_d symmetry. The t_2 orbital is the highest occupied MO, which can be further split by the Jahn–Teller effect, as shown in the PES spectrum of Au_{16}^- in Fig. 1(a). The higher binding energy features beyond 5 eV are due to the gold $5d$ band, whereas the $1s$ and $1p$ shells possess much higher electron binding energies according to Walter and Hakkinen. Thus, the relatively simple spectral pattern due to the $1d$ shell, i.e., the t_2 and e MOs, provides the electronic fingerprint for the T_d cage structure of Au_{16}^- and may be used as experimental

TABLE I. The measured VDEs compared to calculated VDE for the T_d isomers of the doped clusters $M@Au_{16}^-$ (M=Ag,Zn,In).

	VDE (eV)	
	Expt.	Theor.
$Ag@Au_{16}^-$ (T_d)	4.23±0.04	4.34
$Zn@Au_{16}^-$ (T_d)	3.46±0.04	3.38
$In@Au_{16}^-$ (T_d)	3.91±0.04	3.75

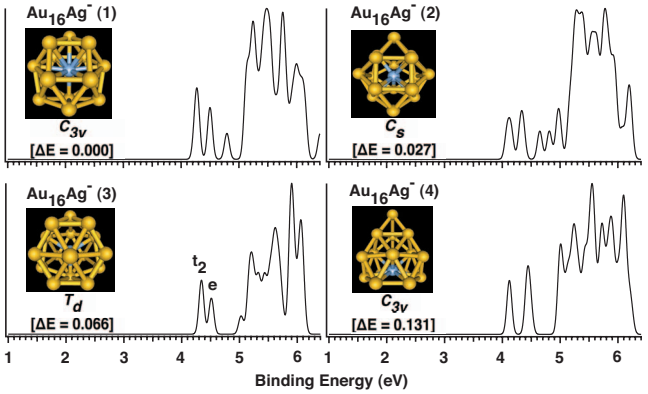

FIG. 2. (Color) Structures, relative energies (ΔE) in eV, and simulated photoelectron spectra for the four low-lying isomers of $Au_{16}Ag^-$.

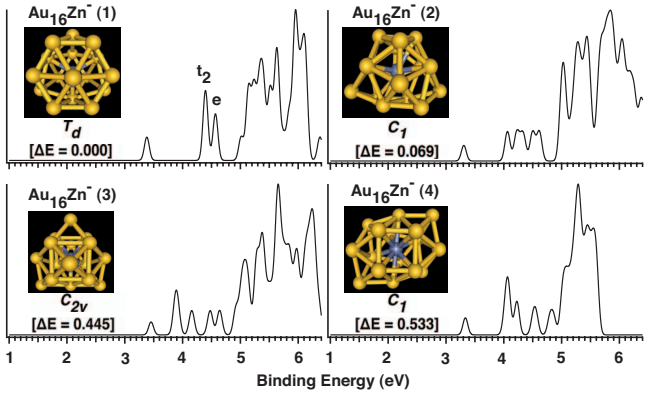

FIG. 3. (Color) Structures, relative energies (ΔE) in eV, and simulated photoelectron spectra for the four low-lying isomers of $Au_{16}Zn^-$.

evidence to judge whether the cage is significantly distorted upon doping.

As shown in Fig. 1, the spectral signatures due to the t_2 and e orbitals can be clearly recognized in the PES spectra of all three doped species, MAu_{16}^- (M=Ag,Zn,In), suggesting that the electronic structures and the near-T_d symmetry of the Au_{16}^- cage are not significantly distorted by the doping, which is possible only if the dopant atoms are trapped inside the cage. The spectrum of $AgAu_{16}^-$ [Fig. 1(b)] is almost identical to that of $CuAu_{16}^-$ because both are 18-electron closed-shell systems and can be viewed as $M^+@Au_{16}^{2-}$. Zn is valence two and can donate two electrons to the Au_{16} cage. Thus, neutral $ZnAu_{16}$ is an 18-electron system isoelectronic to $AgAu_{16}^-$ and $CuAu_{16}^-$. In the $ZnAu_{16}^-$ anion, the extra electron should enter the 2s shell. The large energy gap observed in the spectrum of $ZnAu_{16}^-$ [Fig. 1(c)] suggests that neutral $ZnAu_{16}$ should be a highly stable species. Similarly, indium has three valence electrons and the extra electron should fill up the 2s shell, giving rise to a highly stable 20-electron $InAu_{16}^-$ cage ($1s^21p^61d^{10}2s^2$). The fact that the X band of $InAu_{16}^-$ is more intense and has a higher binding energy than that in the $ZnAu_{16}^-$ spectrum is consistent with the filled 2s shell.

Our theoretical calculations confirmed these observations. The global minimum search revealed that the endohedral cages with T_d symmetry either represent the global minimum structure for the doped clusters ($ZnAu_{16}^-$), or are within less than 0.1 eV from the calculated global minima ($AgAu_{16}^-$ and $InAu_{16}^-$). The simulated PES spectra of the four lowest-lying isomers of MAu_{16}^- (M=Ag,Zn,In) are shown in Figs. 2–4, respectively. For $AgAu_{16}^-$, the lowest energy structure we obtained is a C_{3v} endohedral cage (Fig. 2), which is only slightly distorted from T_d symmetry. However, its simulated PES spectrum shows an additional peak in between the energy gap region, inconsistent with the experimental data. The endohedral T_d cage is the third lowest-lying isomer, about 0.066 eV above the C_{3v} structure. Importantly, the simulated spectrum of the T_d isomer, featuring the characteristic doublet peaks (labeled t_2 and e), agrees well with the experimental data. It should be pointed out that the Jahn–Teller splitting due to detachment from the t_2 orbital cannot be reproduced from our calculations because the geometry was fixed in calculating the first VDE. Considering the uncertainty of the DFT energies for such systems, we conclude that the T_d structure should be assigned as the global minimum for $Ag@Au_{16}^-$. Note that the recent theoretical study[13] that suggested an exohedral $AgAu_{16}^-$ is not supported by the experiment or the current calculation. Our DFT results show that the exohedral $AgAu_{16}^-$ structure is a higher energy isomer and gives a very different PES spectrum.

For $ZnAu_{16}^-$, the global minimum structure we found is the endohedral T_d cage (Fig. 3). Its simulated PES spectrum is in good agreement with the experiment; note again that the Jahn–Teller splitting of the t_2 orbital cannot be reproduced in our current calculation. For $InAu_{16}^-$, the lowest energy structure from our calculations is also a C_{3v} cage (Fig. 4), similar to $AgAu_{16}^-$. However, the T_d isomer is only 0.01 eV higher in energy and yields a simulated spectrum in better agreement with the experiment. Thus, we conclude that the true global minimum of $InAu_{16}^-$ should be the endohedral T_d structure. The calculated first VDEs of the T_d cages for all the three doped clusters are also in good agreement with the experimental data (Table I). The overall agreement between the experimental and theoretical results provides considerable credence for the endohedral structure for $M@Au_{16}^-$ (M=Ag,Zn,In), in which the dopant induces little structural distortion to the parent golden cage.

The observation of the electron filling patterns in the current series of doped $M@Au_{16}^-$ clusters is interesting. It provides experimental evidence that the metal dopant does

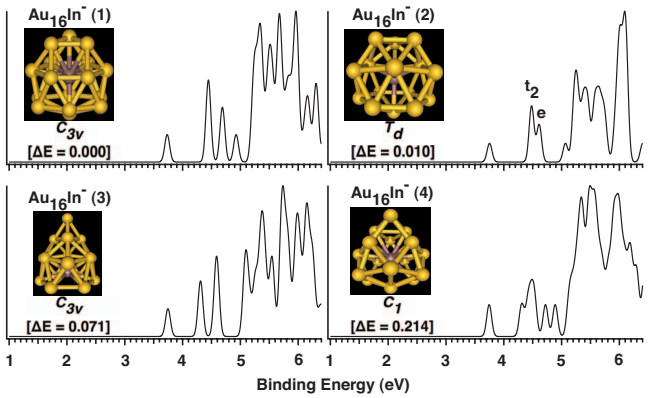

FIG. 4. (Color) Structures, relative energies (ΔE) in eV, and simulated photoelectron spectra for the four low-lying isomers of $Au_{16}In^-$.

not significantly alter the electronic or atomic structure of Au_{16}^-, but simply transfers its valence electrons to the golden cage in $M@Au_{16}^-$, which can be viewed approximately as $Ag^+@Au_{16}^{2-}$, $Zn^{2+}@Au_{16}^{3-}$, and $In^{3+}@Au_{16}^{4-}$. The current work suggests a convenient means to systematically tune the electronic, as well as the chemical and optical, properties of the golden cage by endohedral doping, while maintaining its cage structure. We expect that $Cu@Au_{16}^-$ and $Ag@Au_{16}^-$ would be unreactive to O_2, similar to Au_{16}^-,[26,27] whereas $Zn@Au_{16}^-$ should be reactive to O_2. It would also be interesting to dope the golden cage with transition metals,[28] which may lead to magnetic $M@Au_{16}^-$ clusters. There have been several mass spectrometric studies of gold cluster cations doped with various metal atoms.[29–32] A number of MAu_{16}^+ species with 18 valence electrons have been shown to exhibit higher stability and may assume $M@Au_{16}^+$ type of cage structures. These species and magnetic doping of the golden cages[33] are being actively pursued in our laboratories.

The experimental work was supported by the National Science Foundation (Grant No. CHE-0749496) and performed at the W. R. Wiley Environmental Molecular Sciences Laboratory, a national scientific user facility sponsored by DOE's Office of Biological and Environmental Research and located at Pacific Northwest National Laboratory, operated for DOE by Battelle. The theoretical work was supported in part by grants from the NSF (CHE, CMMI, and DMR/MRSEC), and the Nebraska Research Initiative, and by the Research Computing Facility at University of Nebraska-Lincoln and Holland Supercomputing Center at University of Nebraska-Omaha. X.C.Z. thanks Professor J. M. Dong and Professor W. Fa for helpful discussions.

[1] M. Haruta, Catal. Today **36**, 153 (1997).
[2] S. Bulusu, X. Li, L. S. Wang, and X. C. Zeng, Proc. Natl. Acad. Sci. U.S.A. **103**, 8326 (2006).
[3] H. W. Kroto, J. R. Heath, S. C. O'Brian, R. F. Curl, and R. E. Smalley, Nature (London) **318**, 162 (1985).
[4] Y. Chai, T. Guo, C. Jin, R. E. Haufler, L. P. F. Chibante, J. Fure, L. Wang, J. M. Alford, and R. E. Smalley, J. Phys. Chem. **95**, 7564 (1991).
[5] M. Walter and H. Hakkinen, Phys. Chem. Chem. Phys. **8**, 5407 (2006).
[6] Y. Gao, S. Bulusu, and X. C. Zeng, ChemPhysChem **7**, 2275 (2006).
[7] L. M. Wang, S. Bulusu, H. J. Zhai, X. C. Zeng, and L. S. Wang, Angew. Chem., Int. Ed. **46**, 2915 (2007).
[8] L. M. Wang, S. Bulusu, W. Huang, R. Pal, L. S. Wang, and X. C. Zeng, J. Am. Chem. Soc. **129**, 15136 (2007).
[9] Q. Sun, Q. Wang, G. Chen, and P. Jena, J. Chem. Phys. **127**, 214706 (2007).
[10] Q. Sun, Q. Wang, P. Jena, and Y. Kawazoe, ACS Nano **2**, 341 (2008).
[11] P. Pyykkö and N. Runeberg, Angew. Chem., Int. Ed. **41**, 2174 (2002).
[12] X. Li, B. Kiran, J. Li, H. J. Zhai, and L. S. Wang, Angew. Chem., Int. Ed. **41**, 4786 (2002).
[13] W. Fa and J. M. Dong, J. Chem. Phys. **128**, 144307 (2008).
[14] T. Guo, R. E. Smalley, and G. E. Scuseria, J. Chem. Phys. **99**, 352 (1993).
[15] L. S. Wang, H. S. Cheng, and J. W. Fan, J. Chem. Phys. **102**, 9480 (1995).
[16] D. J. Wales and H. A. Scheraga, Science **285**, 1368 (1999).
[17] D. J. Wales and J. P. K. Doye, J. Phys. Chem. A **101**, 5111 (1997).
[18] S. Yoo and X. C. Zeng, Angew. Chem., Int. Ed. **44**, 1491 (2005).
[19] J. P. Perdew, K. Burke, and M. Ernzerhof, Phys. Rev. Lett. **77**, 3865 (1996).
[20] DMOL3 is a density functional theory program distributed by Accelrys, Inc.; B. Delley, J. Chem. Phys. **92**, 508 (1990).
[21] P. J. Hay and W. R. Wadt, J. Chem. Phys. **82**, 299 (1985).
[22] M. J. Frisch, G. W. Trucks, H. B. Schlegel *et al.*, GAUSSIAN 03, Revision C.02, Gaussian, Inc., Wallingford CT, 2004.
[23] K. J. Taylor, C. L. Pettiettehall, O. Cheshnovsky, and R. E. Smalley, J. Chem. Phys. **96**, 3319 (1992).
[24] H. Hakkinen, B. Yoon, U. Landman, X. Li, H. J. Zhai, and L. S. Wang, J. Phys. Chem. A **107**, 6168 (2003).
[25] J. Li, X. Li, H. J. Zhai, and L. S. Wang, Science **299**, 864 (2003).
[26] B. E. Salisbury, W. T. Wallace, and R. L. Whetten, Chem. Phys. **262**, 131 (2000).
[27] Y. D. Kim, M. Fischer, and G. Gantefor, Chem. Phys. Lett. **377**, 170 (2003).
[28] X. Li, B. Kiran, L. F. Cui, and L. S. Wang, Phys. Rev. Lett. **95**, 253401 (2005).
[29] M. Heinebrodt, N. Malinowski, F. Tast, W. Branz, I. M. Billas, and T. P. Martin, J. Chem. Phys. **110**, 9915 (1999).
[30] W. Bouwen, F. Vanhoutte, F. Despa, S. Bouckaert, S. Neukermans, L. T. Kuhn, H. Weidele, P. Lievens, and R. E. Silverans, Chem. Phys. Lett. **314**, 227 (1999).
[31] S. Neukermans, E. Janssens, H. Tanaka, R. E. Silverans, and P. Lievens, Phys. Rev. Lett. **90**, 033401 (2003).
[32] N. Veldeman, E. Janssens, K. Hansen, J. D. Haeck, R. E. Silverans, and P. Lievens, Faraday Discuss. **138**, 147 (2008).
[33] L. M. Wang, J. Bai, A. Lechtken, W. Huang, D. Schooss, M. M. Kappes, X. C. Zeng, and L. S. Wang, Phys. Rev. B (unpublished).